Electronic Supplementary Information

Turn-on fluorescent capsule for selective fluoride detection and water purification

Yannan Lin, Kang Du, Michael R. Gau, and Ivan J. Dmochowski*

Department of Chemistry, University of Pennsylvania, 231 S. 34th St., Philadelphia, Pennsylvania 19104–6323, United States

Table of Contents

General Considerations

Unless otherwise specified, chemicals and solvents were purchased from commercial vendors and used without purification. [3H-***L***][OMs]$_3$ was prepared according to a literature procedure.[1] ^{1}H NMR and ^{19}F NMR spectra were recorded on a NEO600 NMR spectrometer at 298 K and chemical shifts were reported in ppm. Fluorescence spectra were measured at 298 K in 1-cm path length quartz cuvettes using a Varian Cary Eclipse fluorescence spectrometer. UV-vis spectra were measured at 298 K in 1-cm path length quartz cuvettes using a Cary 3500 UV-vis spectrometer. Solution pH measurements were made using a Fisherbrand accumet AE150 benchtop pH meter with an Oakton glass-body combination pH electrode. For NMR measurements, the pD was maintained at pD 4.5 ± 0.1 and adjusted with a concentrated solution of methanesulfonic acid or sodium hydroxide in D_2O. For fluorescence measurements in pure H_2O and D_2O, the pH was maintained at pH 4.1 ± 0.1 and the pD was maintained at pD 4.5 ± 0.1, both of which were achieved by adjusting the sample solutions with a concentrated solution of methanesulfonic acid or sodium hydroxide in H_2O or D_2O.

Acid-Based Titration

Due to the poor solubility of the capsule in pure water at pH higher than 8, the titration was performed in a solvent mixture of H_2O/MeOH (1:1 *v*/*v*). CO_2 was excluded from DI water by freshly boiling for 15 min and cooling under nitrogen, and excluded from methanol by vigorous nitrogen bubbling for 15 min before use. During the whole experiment, the titration cell was protected under a nitrogen atmosphere. In a typical experiment, aliquots of carbonate-free NaOH (50 mM) were titrated with a microliter pipetman to the solution of [3H-***L***][OMs]$_3$ (40 mL, 100 μM) which also contains excess methanesulfonic acid (5 mM) and sodium methanesulfonate (95 mM) to maintain the total ionic strength. The pH values were recorded 1 min afterwards with stirring over a pH range of 2.29–11.05 at 298 K. A titration curve was created by plotting the pH values that were measured against the total volume of NaOH that was titrated (**Figure S1**). To calculate the pK_a values, the second derivative of the titration curve was generated (**Figure S2**), in which the first (V_1), third (V_2) and fifth *x*-intercept (V_3) corresponded to the first, second and third equivalence points of the titration.[2] On the basis of this graph, the second half equivalence point was determined from the midpoint between the first and second equivalence points ($\frac{V_1 + V_2}{2}$), and the third half equivalence point was determined from the midpoint between the second and third equivalence points ($\frac{V_2 + V_3}{2}$). The volume of NaOH that neutralized half equivalence of the capsule (V_{half}) was estimated by taking the difference between the first and third equivalence points ($V_3 - V_1$) and dividing by four ($V_{\text{half}} \approx \frac{(V_3 - V_1)}{4}$). The first half equivalence point was determined from V_4, which was estimated to be $V_4 = V_1 - V_{\text{half}}$. The p*K*a values were reported in **Table S1**, and the protonation species distribution diagram was presented as **Figure S3** using the HYSS program.

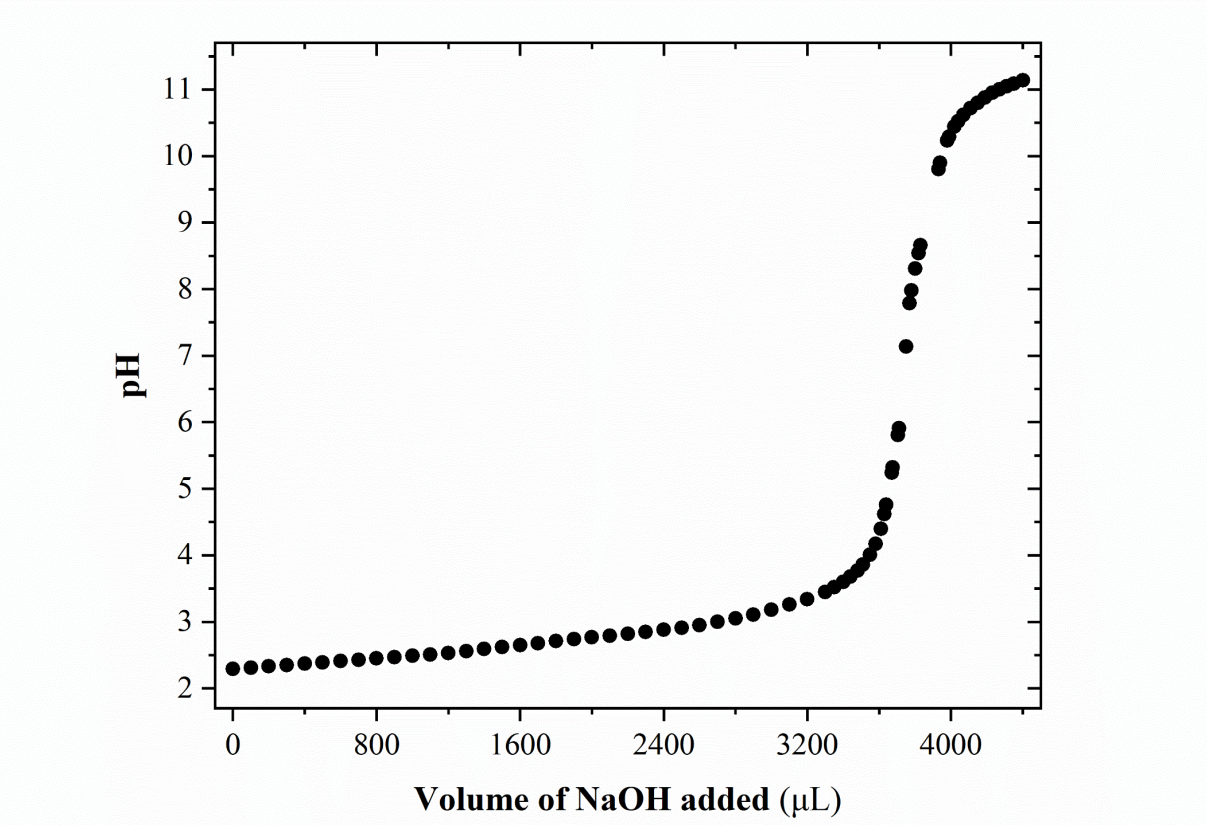

Figure S1. Titration curve of [3H-***L***][OMs]$_3$ using 50 mM carbonate-free NaOH in H_2O/MeOH (1:1 *v*/*v*).

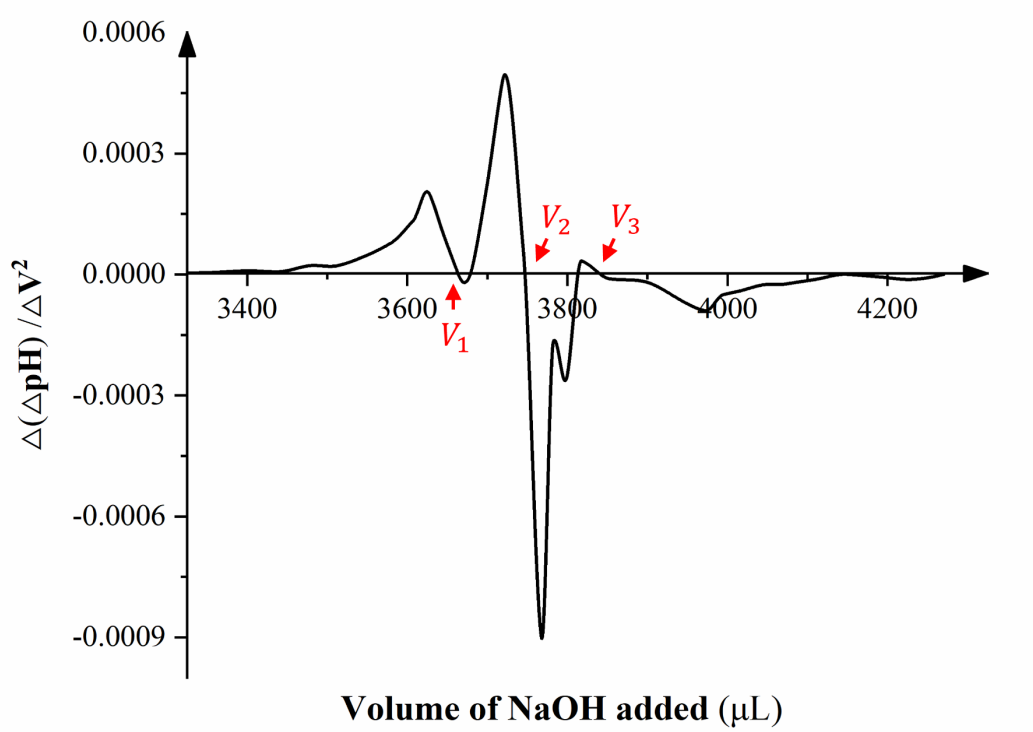

Figure S2. The second derivative of the titration curve. V_1, V_2 and V_3 represent the first, third, and fifth *x*-intercepts, respectively.

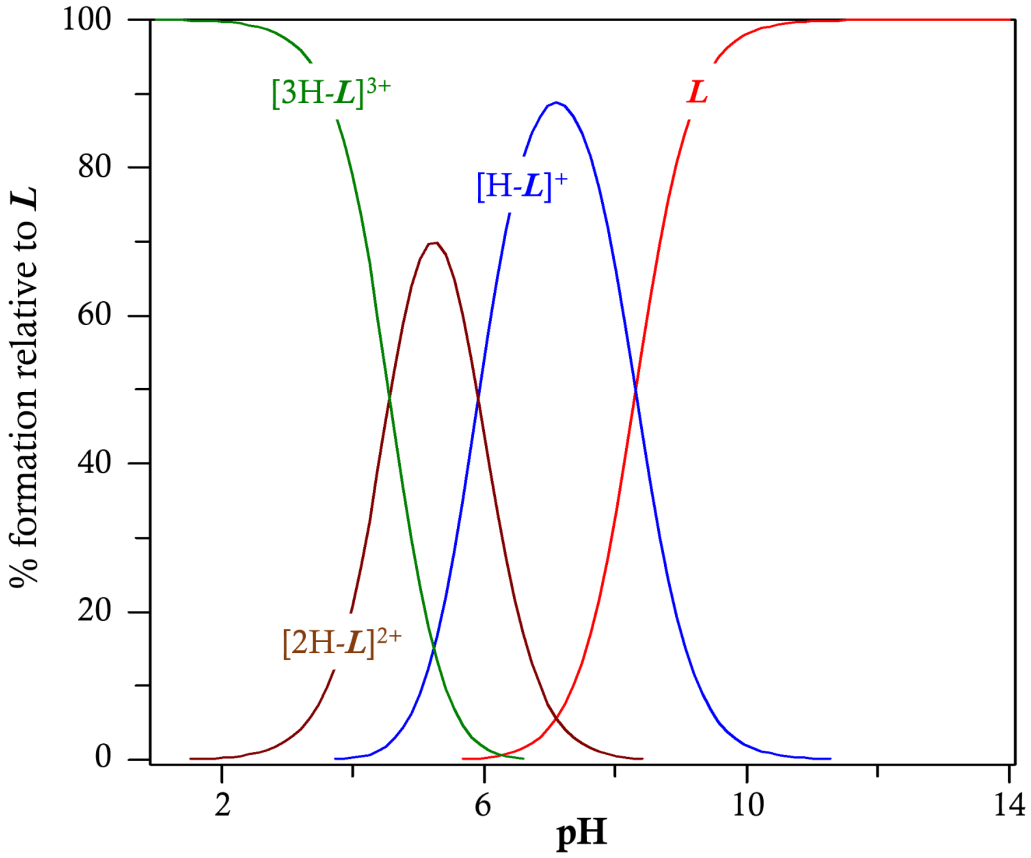

Figure S3. Species distribution diagram for hemicryptophane (0.1 M) as a function of pH in H_2O/MeOH (1:1 *v*/*v*).

Table S1. Stepwise dissociation constants (K_a) of [3H-***L***][OMs]$_3$ in H_2O/MeOH (1:1 *v*/*v*).

Dissociation	$-\log_{10} K_a$ (pK_a)
$[3H\text{-}\boldsymbol{L}]^{3+} \rightleftharpoons [2H\text{-}\boldsymbol{L}]^{2+} + H^+$	4.57
$[2H\text{-}\boldsymbol{L}]^{2+} \rightleftharpoons [H\text{-}\boldsymbol{L}]^{+} + H^+$	5.91
$[H\text{-}\boldsymbol{L}]^{+} \rightleftharpoons \boldsymbol{L} + H^+$	8.31

NMR Spectral Data

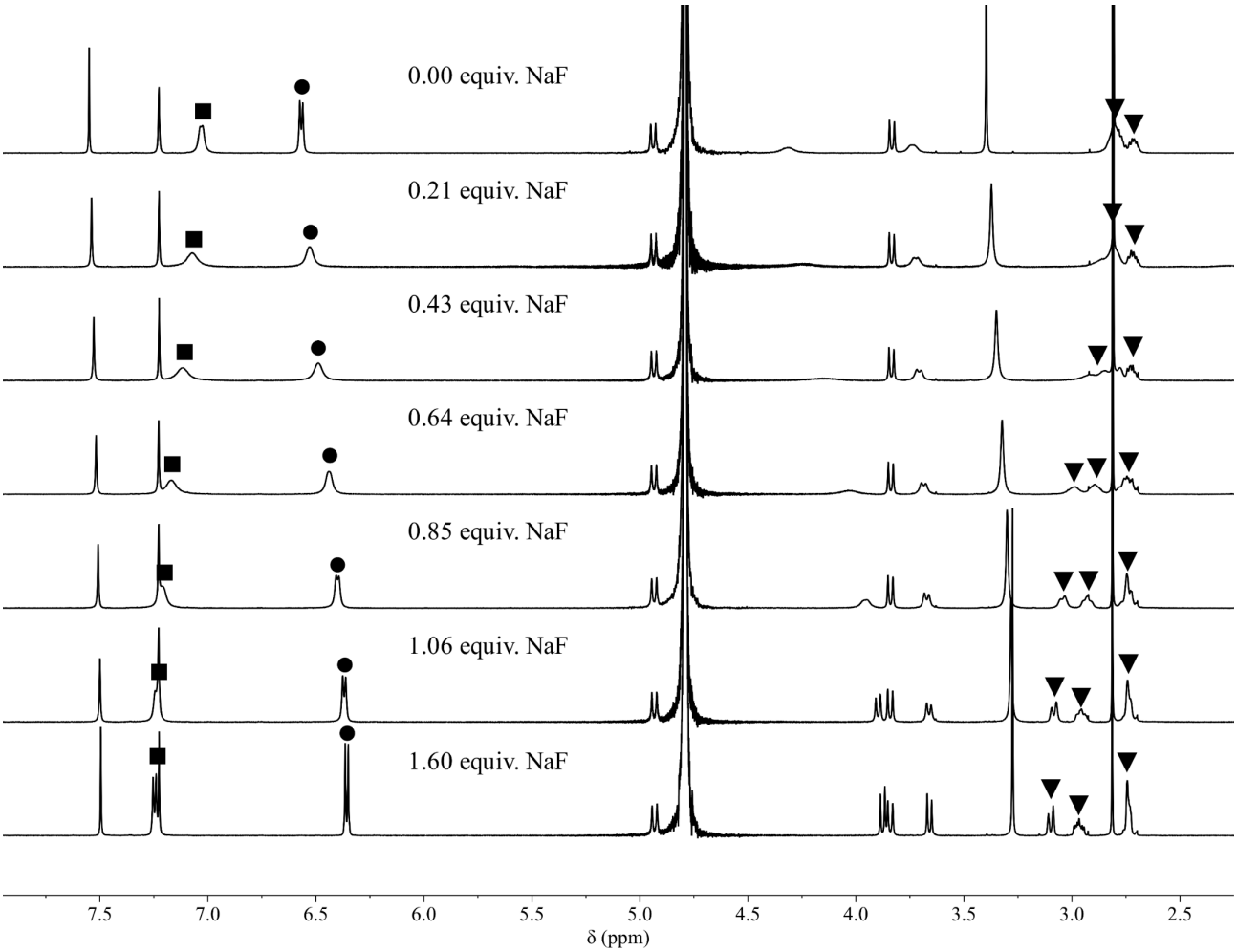

Figure S4. ^{1}H NMR spectra (600 MHz, 298 K, D_2O) recorded during the titration of 0.5 mM [3H-***L***][OMs]$_3$ with NaF at pD 4.5 ± 0.1. ▼: proton signals assigned to H_a, H_b, H_c and H_d; ●: proton signals assigned to H_e; ■: proton signals assigned to H_f.

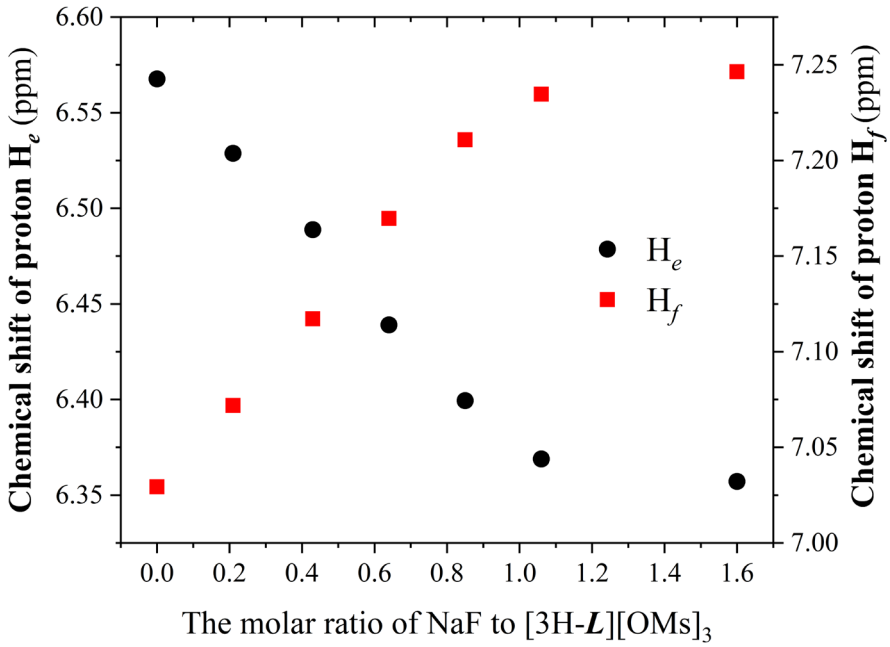

Figure S5. Titration curve between [3H-***L***][OMs]$_3$ and NaF in D_2O at pD 4.5 ± 0.1. The chemical shifts (δ) of protons H_e and H_f on the *p*-phenylene linkers are plotted as a function of molar ratio of NaF to [3H-***L***][OMs]$_3$. The black spheres and red squares represent the chemical shifts (δ) of protons H_e and H_f, respectively.

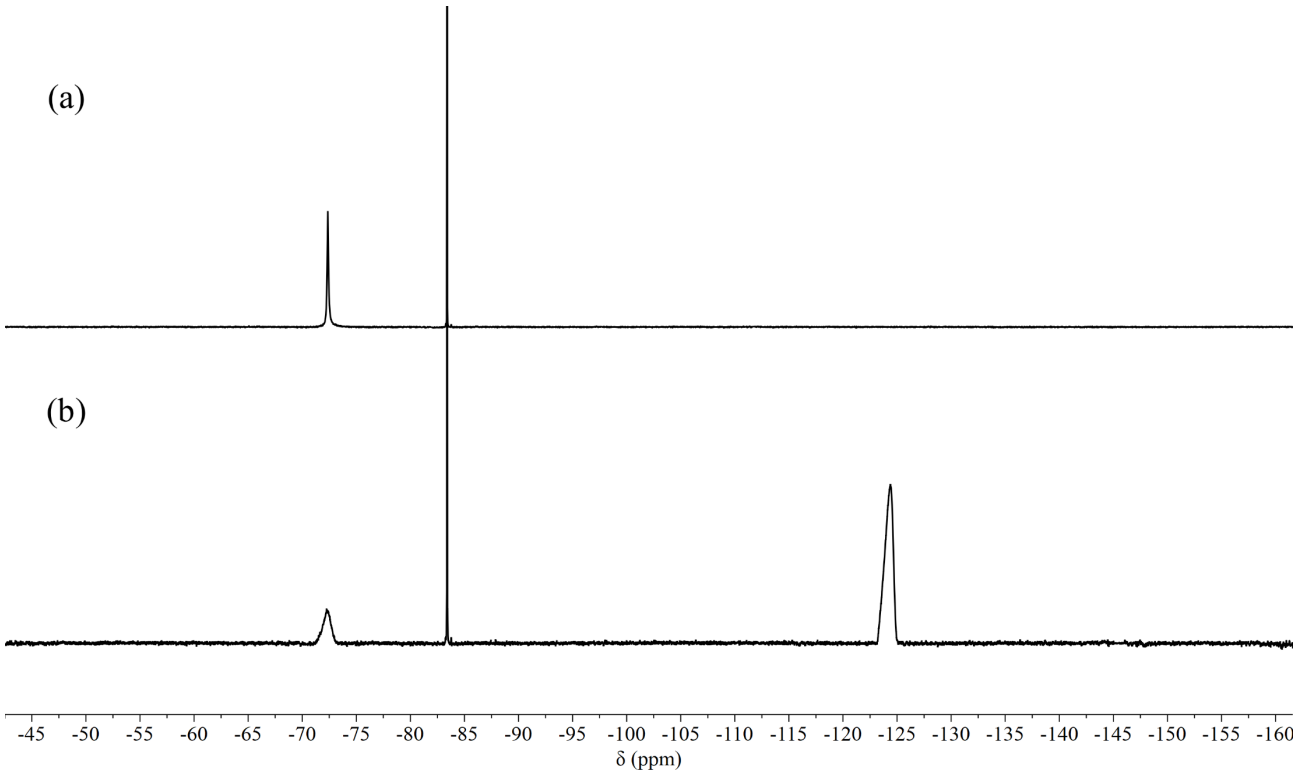

Figure S6. Extended ^{19}F NMR spectra (565 MHz, 298 K, D_2O, pD 4.5 ± 0.1, hexafluoroacetone as internal reference) of (a) 1.5 mM [3H-***L***][OMs]$_3$ (2 *eq*.) with 0.75 mM NaF (1 *eq*.); (b) 1.5 mM [3H-***L***][OMs]$_3$ (2 *eq*.) with 4.5 mM NaF (6 *eq*.). No signal was detected in the range of 140–160 ppm, confirming the absence of any additional fluoride species such as HF or HF_2^- throughout the experiment.

Crystallographic Data

Single crystal X-ray diffraction data were collected on a Rigaku XtaLAB Synergy-S diffractometer with hybrid pixel array detector using confocal multilayer optic-monochromated Cu-Kα radiation (λ = 1.54184 Å), integrated using *CrysAlisPro* (Rigaku Oxford Diffraction, version 1.171.40.104a, 2020) and corrected for absorption using *SCALE3 ABSPACK* (Rigaku Oxford Diffraction, version 1.0.7, 2005). The structure was solved by dual space methods – *SHELXT*.[3] There were regions of disordered solvent for which reliable disorder models could not be devised; the X-ray data were corrected for the presence of disordered solvent using *SQUEEZE*.[4] Refinement was by full-matrix least squares based on F^2 using *SHELXL*.[5] Non-hydrogen atoms were refined anisotropically and hydrogen atoms were refined using a riding model. During refinement, fixing the stoichiometry of two methanesulfonates per ***L*** resulted in poor fits. One possible explanation is that a small portion of triply deprotonated ***L*** were partially deprotonated due to the presence of excess NaF and change of pH in organic solvents used for crystallization. Therefore, the occupancy of the anion was allowed to refine freely to give 1.6 methanesulfonates per ***L*** with satisfactory refinement parameters. This is consistent with the hypothesis that a small amount of ***L*** is not triply deprotonated in the crystals. The empirical formula is therefore adjusted accordingly as indicated in Table S2. Note that this observation doesn't alter any solution analyses in the main text, as they were carried out at closely monitored pH and the methanesulfonates are anticipated to be fully dissociated in aqueous solutions.

Table S2. Crystallographic data for [F•2.6H-***L***][OMs]$_{1.6}$·H_2O·1.6MeOH (CCDC-2171670).

	[F•2.6H-***L***][OMs]$_{1.6}$·H_2O·0.4MeOH
Empirical formula	$C_{54}H_{68}FN_4O_{13.2}S_{1.6}$
Formula weight, g·mol^{-1}	1054.62
Crystal system	Trigonal
Space group	$R\bar{3}$
Wavelength, Å	1.54184
Temperature, K	100
a, Å	11.71560(10)
c, Å	76.4420(6)
Volume, Å^3	9086.39(17)
Z	6
Density (calculated), Mg·m^{-3}	1.156
Absorption coefficient, mm^{-1}	1.192
F(000)	3361.0
Crystal size, mm	0.12 × 0.1 × 0.02
2θ range for data collection, °	6.938–148.872
Index ranges	$-14 \le h \le 14$, $-14 \le k \le 14$, $-82 \le l \le 95$
Reflections collected	49635
Independent reflections	4149 [*R*(int) = 0.0366]
Data / restraints / parameters	4149 / 268 / 319
Goodness-of-fit on F^2	1.050
Final *R* indexes ($I > 2\sigma$(I))	R_1 = 0.0881, wR_2 = 0.2744
Final *R* indexes (all data)	R_1 = 0.0914, wR_2 = 0.2794
Largest diff. peak and hole	0.61 and –0.29 e·Å^{-3}

Fluorescence Spectral Data

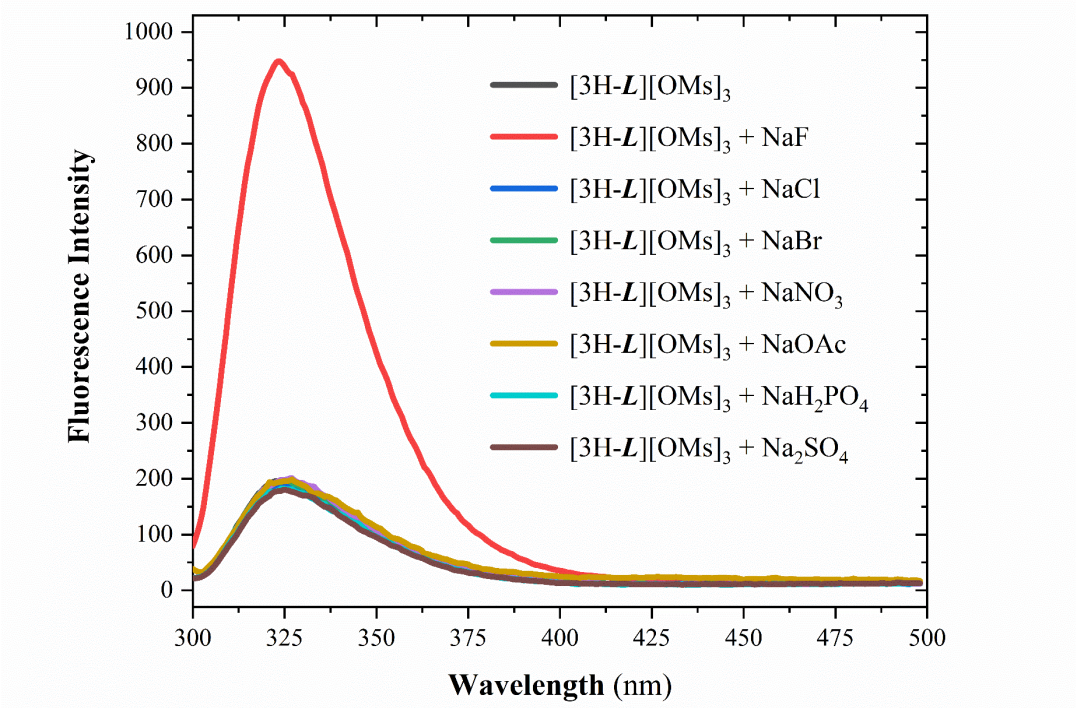

Figure S7. Fluorescence spectra at 298 K of an aqueous solution of 25 μM [3H-***L***][OMs]$_3$ with 10 *eq*. different anions titrated in H_2O at pH 4.1 ± 0.1.

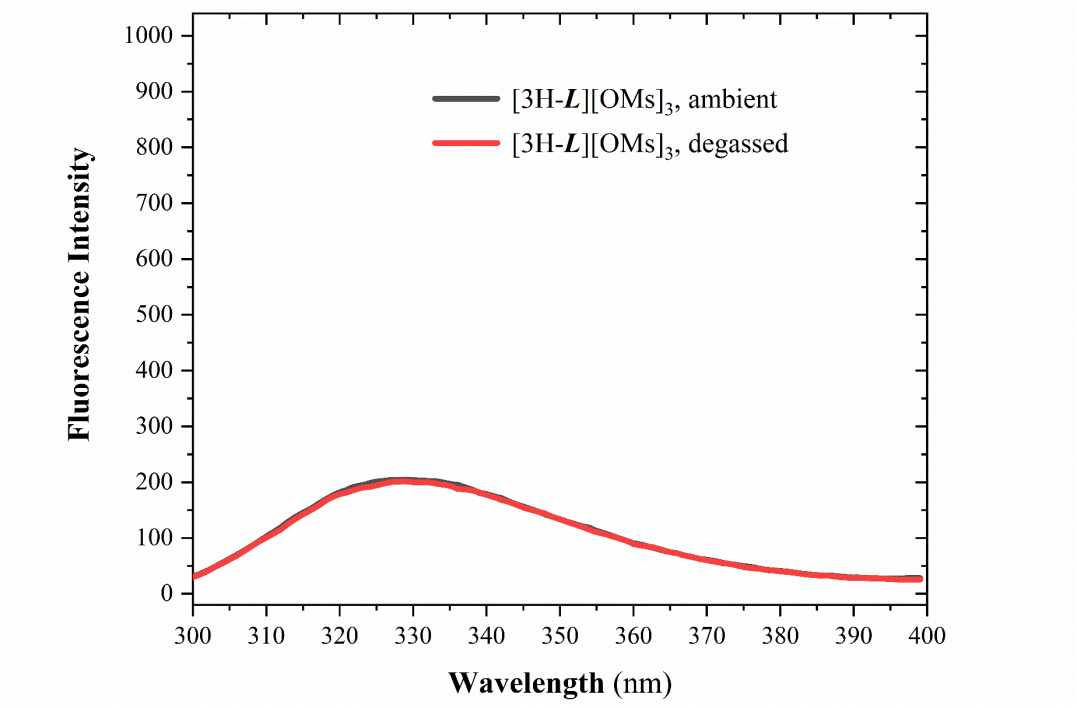

Figure S8. Fluorescence spectra at 298 K of a solution of 25 μM [3H-***L***][OMs]$_3$ under ambient and deaerated condition in H_2O at pH 4.1 ± 0.1.

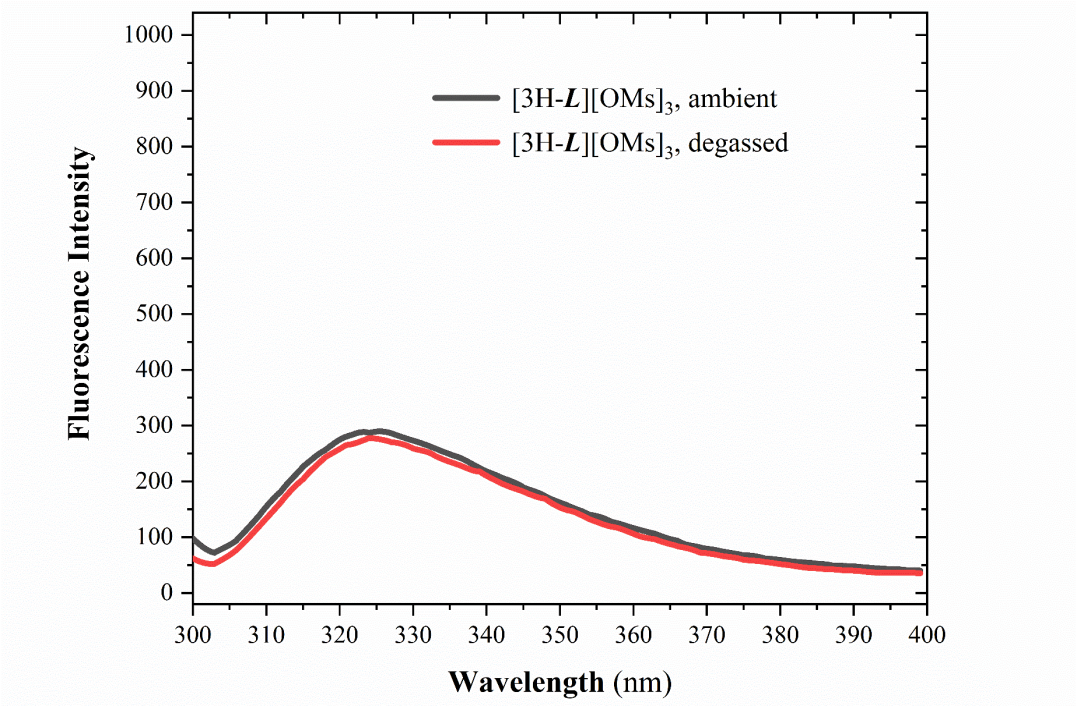

Figure S9. Fluorescence spectra at 298 K of a solution of 15 μM [3H-***L***][OMs]$_3$ under ambient and deaerated condition in citrate buffer (0.1 M, H_2O) at pH 4.1.

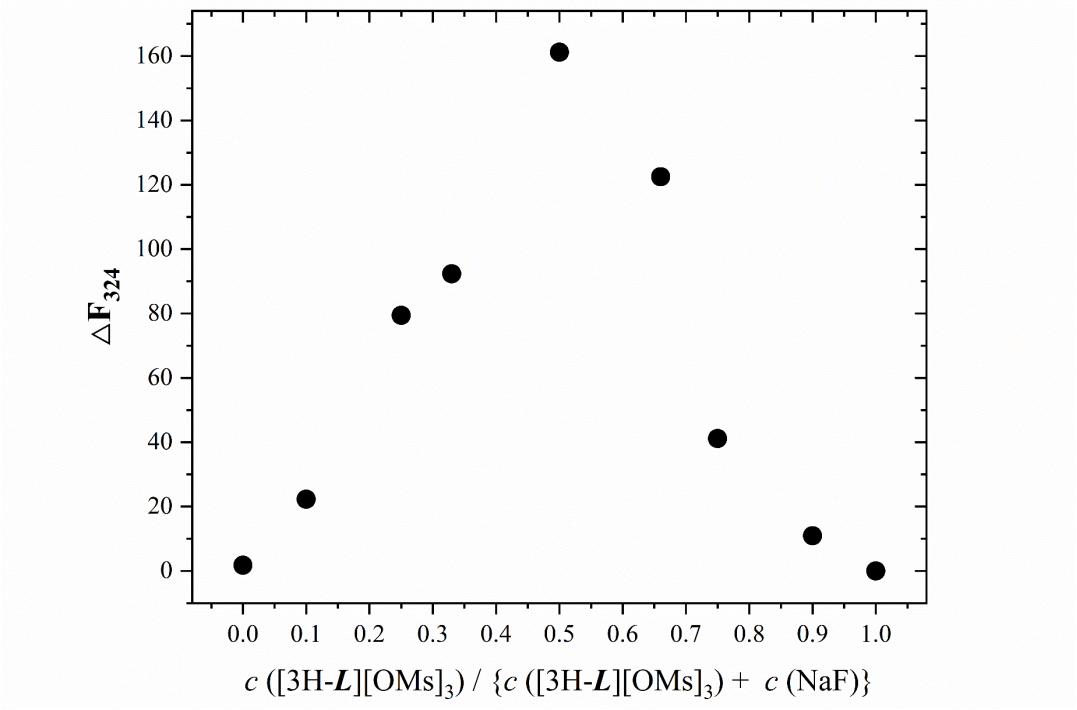

Figure S10. Job plot analysis of the hemicryptophane-fluoride host-guest system at 298 K in citrate buffer (0.1 M, H_2O) at pH 4.1. $\triangle F_{324}$ = fluorescence difference of [3H-***L***][OMs]$_3$ with and without F^- at λ_{max} = 324 nm at 298 K. *c* ([3H-***L***][OMs]$_3$) + *c* (NaF) = 50 μM.

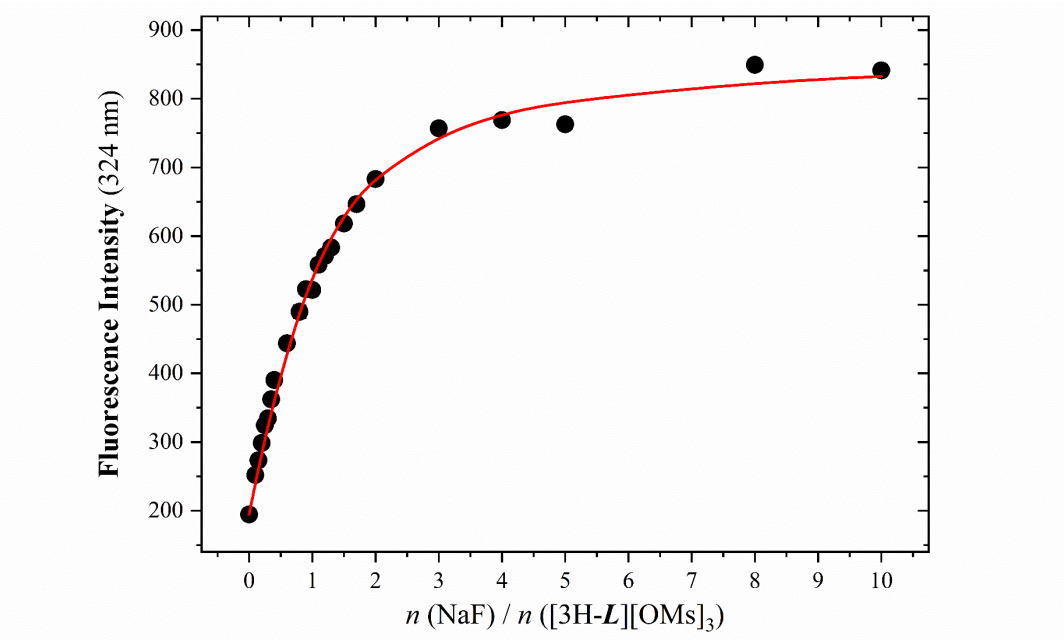

Figure S11. Titration curve between 15 μM [3H-***L***][OMs]$_3$ and NaF at 298 K in citrate buffer (0.1 M, D_2O, 298 K) at pD 4.5. The fluorescence intensity at 324 nm is plotted as a function of the equivalents of added NaF. The black spheres and red line represent experimental data and a global fit, respectively. The error bars represent standard deviations obtained from averaging three measurements. The association constant K_A was calculated to be (1.4 ± 0.1) × 10^5 M^{-1}.

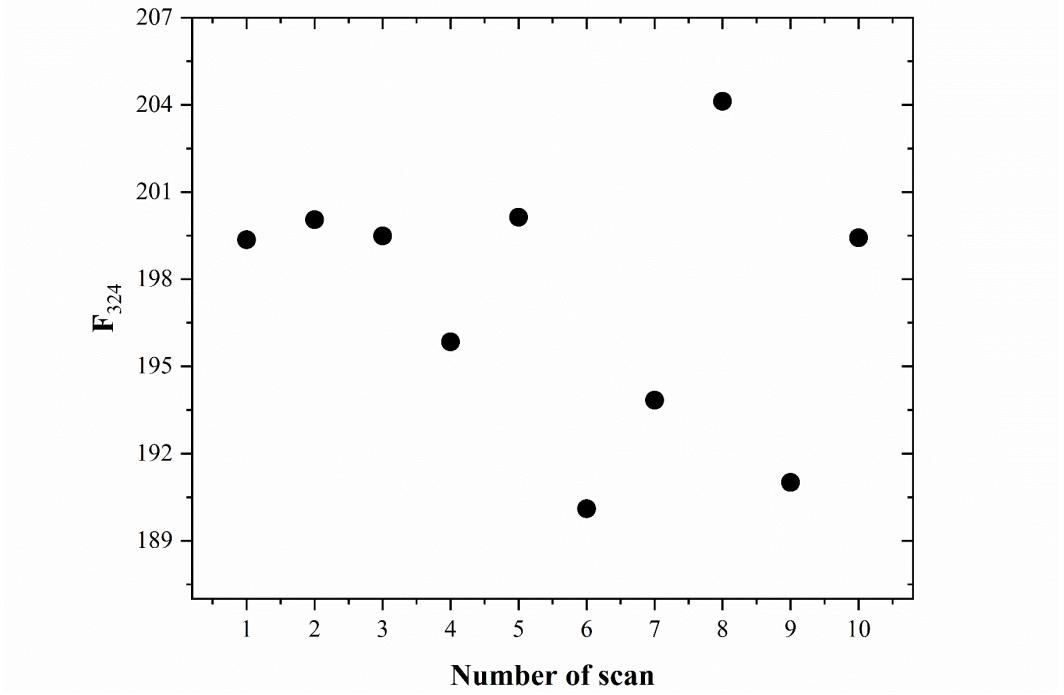

Figure S12. Fluorescence intensities at 324 nm of ten identical scans at 298 K on 15 μM [3H-***L***][OMs]$_3$ in citrate buffer (0.1 M, H_2O) at pH 4.1. The standard deviation (σ) of these ten measurements was 4.5.

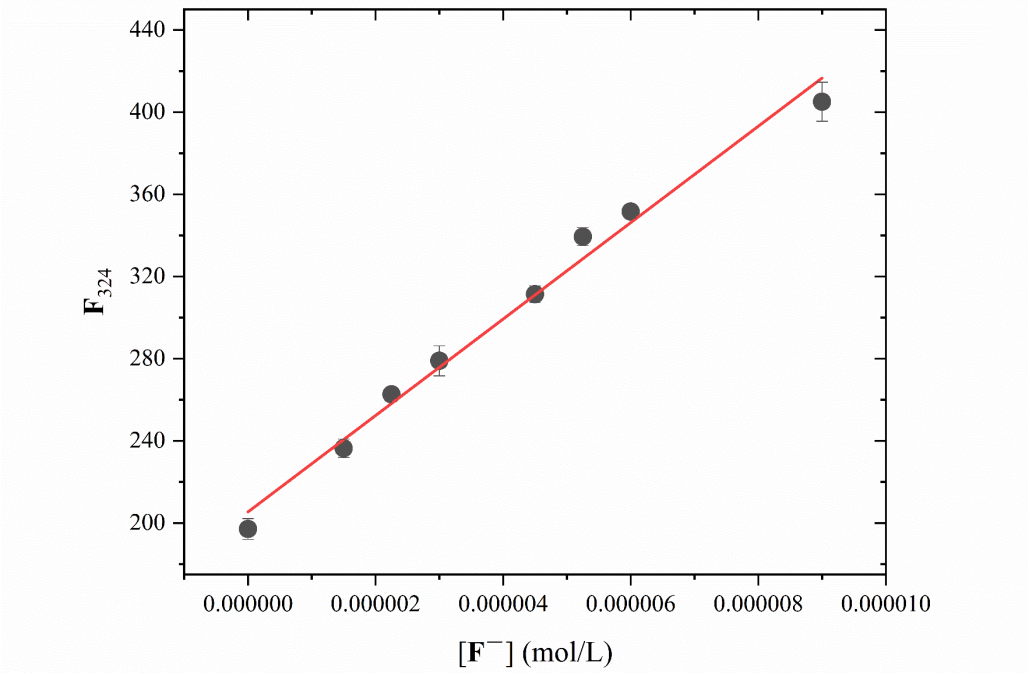

Figure S13. Fluorescence changes at 324 nm of 15 μM [3H-***L***][OMs]$_3$ versus F^- concentration at 298 K in citrate buffer (0.1 M, H_2O) at pH 4.1. The black spheres and red line represent experimental data and a linear fit, respectively. The error bars represent standard deviations obtained from averaging three measurements. The slope of linear calibration plot (k) was calculated to be 2.35×10^7 M^{-1} ($R^2 = 0.988$). To calculate the detection limit (LOD), equation LOD = $3\sigma/k$ was used,[6] which gave 0.6 μM.

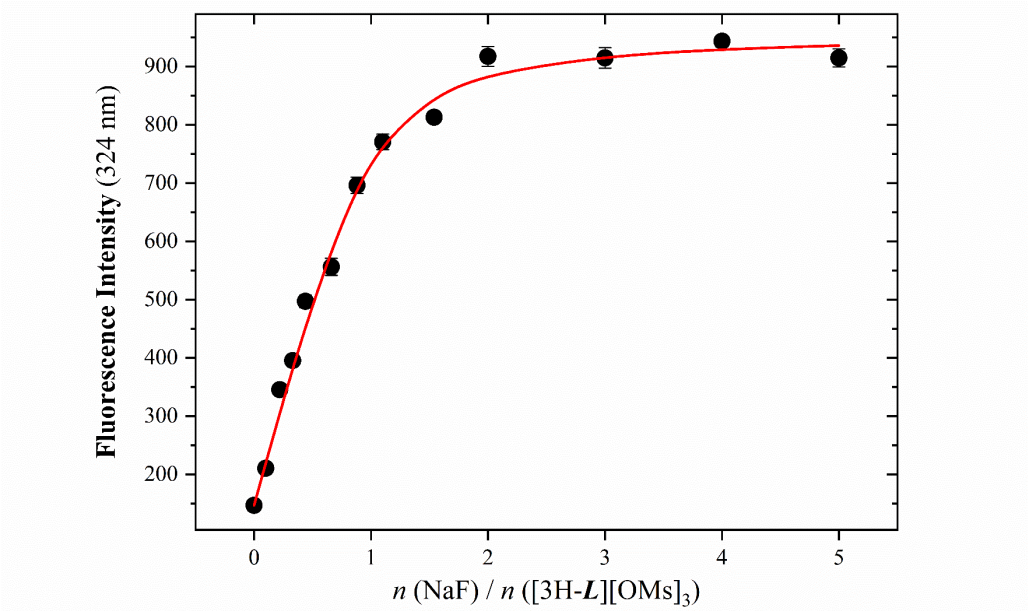

Figure S14. Titration curve between 25 μM [3H-***L***][OMs]$_3$ and NaF at 298 K in H_2O at pH 4.1 ± 0.1. The fluorescence intensity at 324 nm is plotted as a function of the equivalents of added NaF. The black spheres and red line represent experimental data and global fit, respectively. The error bars represent standard deviations obtained from averaging three measurements. The association constant K_A was calculated to be $(4.0 \pm 1.3) \times 10^5$ M^{-1}.

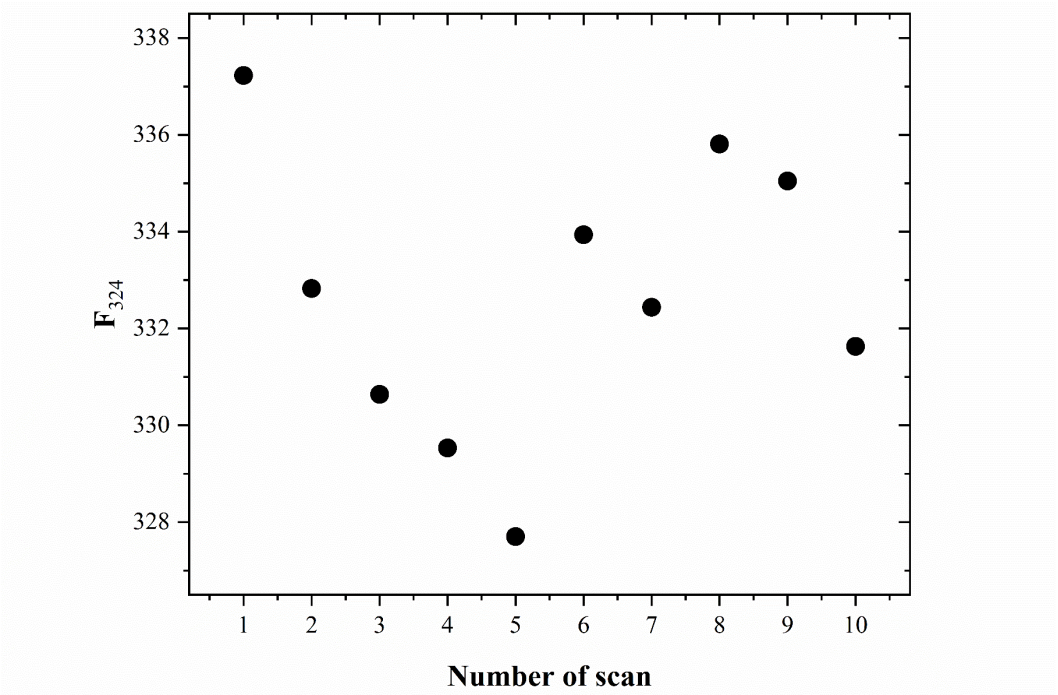

Figure S15. Fluorescence intensities at 324 nm of ten identical scans at 298 K on 15 μM [3H-***L***][OMs]$_3$ in H_2O at pH 4.1 ± 0.1. The standard deviation (σ) of these ten measurements was 2.9.

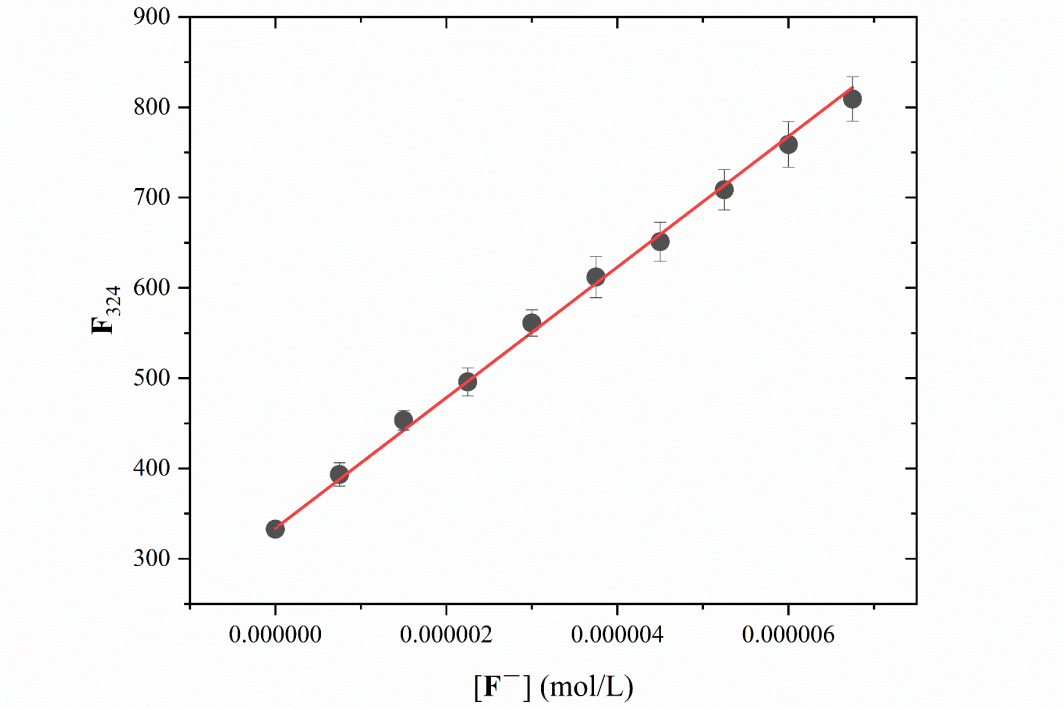

Figure S16. Fluorescence changes at 324 nm of 25 μM [3H-***L***][OMs]$_3$ versus F^- concentration at 298 K in H_2O at pH 4.1 ± 0.1. The black spheres and red line represent experimental data and a linear fit, respectively. The error bars represent standard deviations of averaging three measurements. The slope of linear calibration plot (k) was calculated to be 7.23×10^7 M^{-1} ($R^2 = 0.998$). To calculate detection limit, equation LOD = $3\sigma/k$ was used,[6] which gave 0.1 μM.

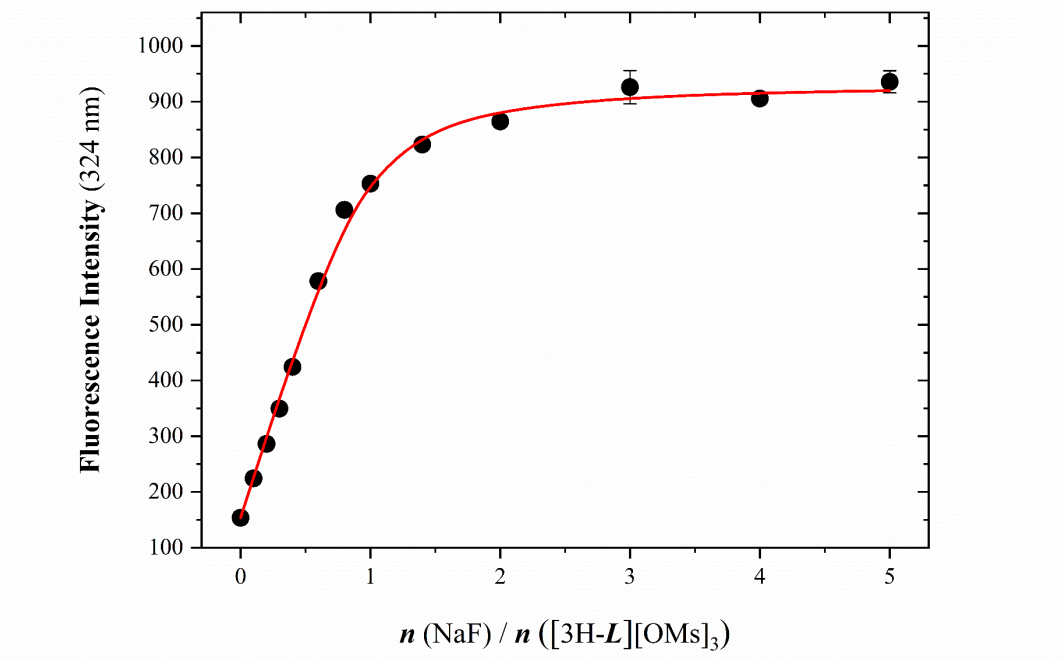

Figure S17. Titration curve between 25 μM [3H-***L***][OMs]$_3$ and NaF at 298 K in D_2O at pD 4.5 ± 0.1. The fluorescence intensity at 324 nm is plotted as a function of the equivalents of added NaF. The black spheres and red line represent experimental data and global fit, respectively. The error bars represent standard deviations of averaging three measurements. The association constant K_A was calculated to be (6.0 ± 1.7) × 10^5 M^{-1}.

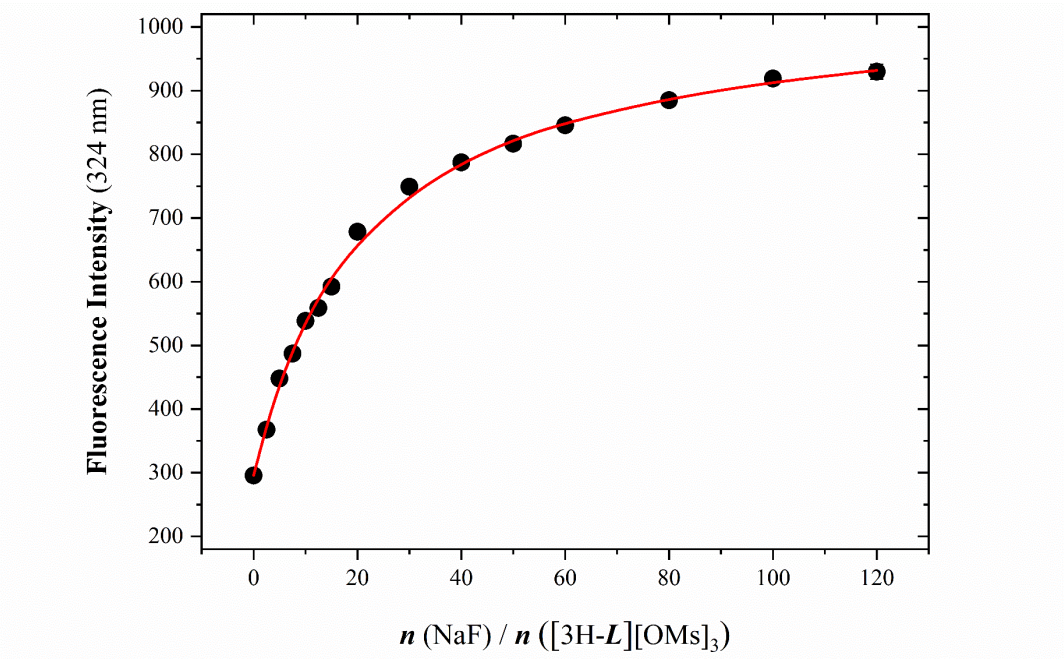

Figure S18. Titration curve between 15 μM [3H-***L***][OMs]$_3$ and NaF at 298 K in citrate buffer (0.1 M, H_2O) at pH 7.0. The fluorescence intensity at 324 nm is plotted as a function of the equivalents of added NaF. The black spheres and red line represent experimental data and a global fit, respectively. The error bars represent standard deviations of averaging three measurements. The association constant K_A was calculated to be (3.2 ± 0.1) × 10^3 M^{-1}.

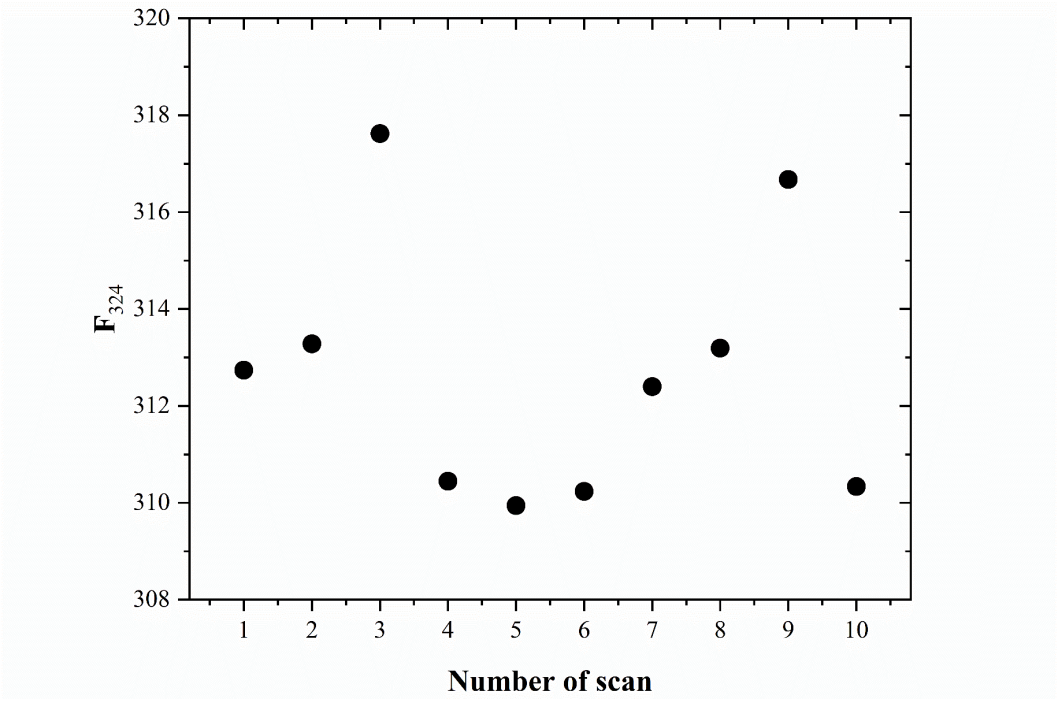

Figure S19. Fluorescence intensities at 324 nm of ten identical scans at 298 K on 15 μM [3H-***L***][OMs]$_3$ in citrate buffer (0.1 M, H_2O) at pH 7.0. The standard deviation (σ) of these ten measurements was 2.7.

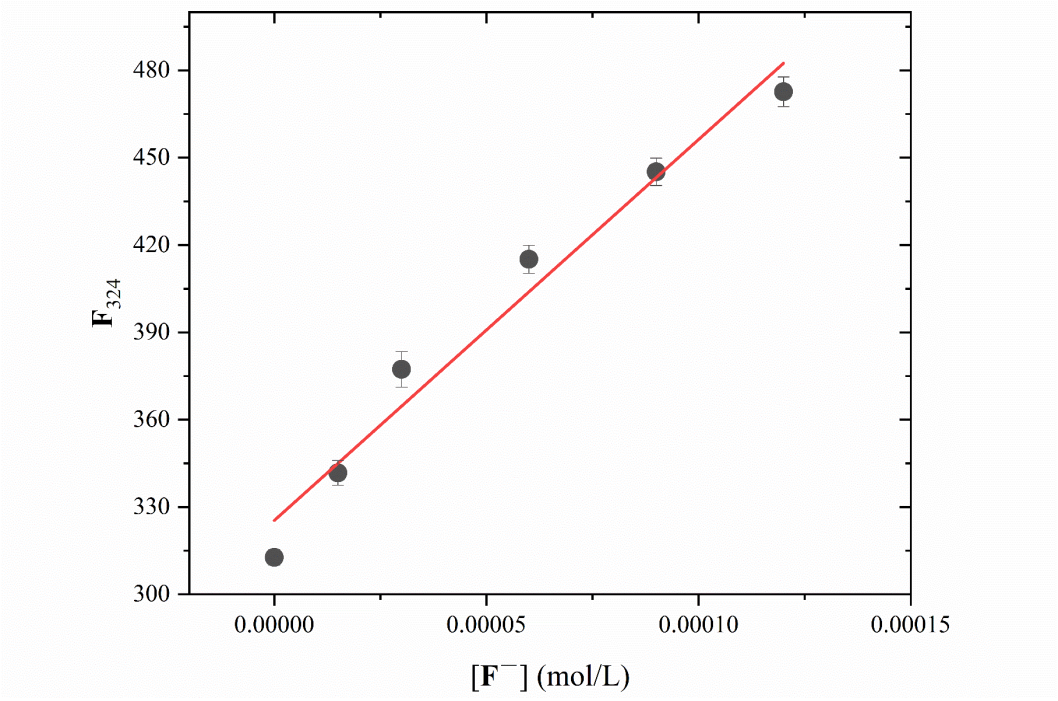

Figure S20. Fluorescence changes at 324 nm of 15 μM [3H-***L***][OMs]$_3$ versus F^- concentration at 298 K in citrate buffer (0.1 M, H_2O) at pH 7.0. The black spheres and red line represent experimental data and a linear fit, respectively. The error bars represent standard deviations obtained from averaging three measurements. The slope of linear calibration plot (k) was calculated to be 1.31×10^6 M^{-1} ($R^2 = 0.970$). To calculate the detection limit, equation LOD = $3\sigma/k$ was used,[6] which gave 6.2 μM.

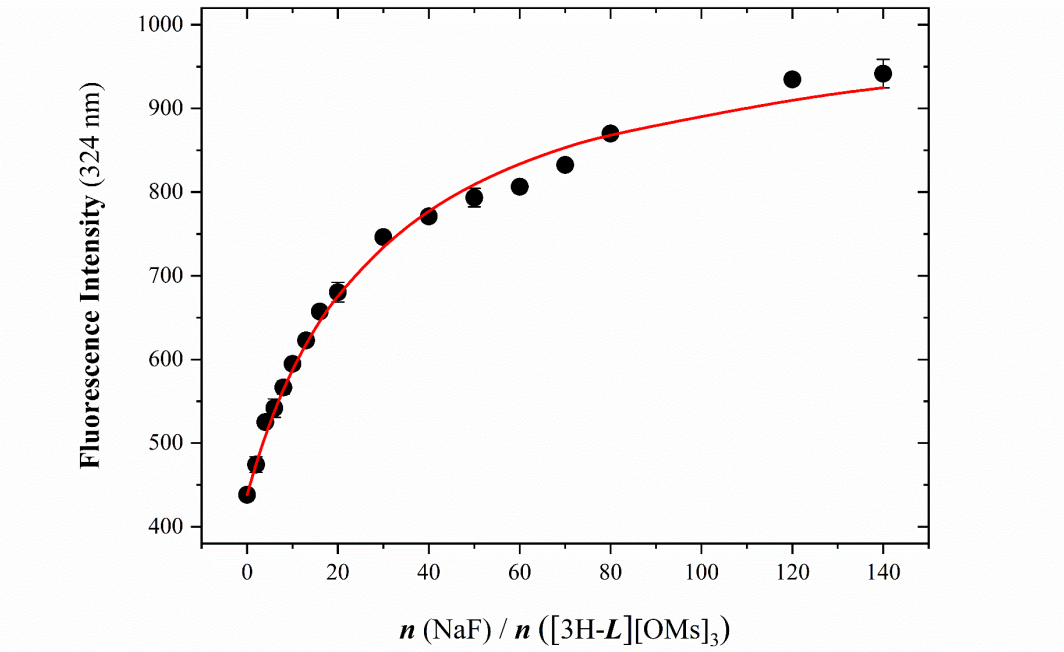

Figure S21. Titration curve between 15 μM [3H-***L***][OMs]$_3$ and NaF at 298 K in PBS (10×, H_2O) at pH 7.0. The fluorescence intensity at 324 nm is plotted as a function of the equivalents of added NaF. The black spheres and red line represent experimental data and a global fit, respectively. The error bars represent standard deviations obtained from averaging three measurements. The association constant K_A was calculated to be $(2.3 \pm 0.2) \times 10^3$ M^{-1}.

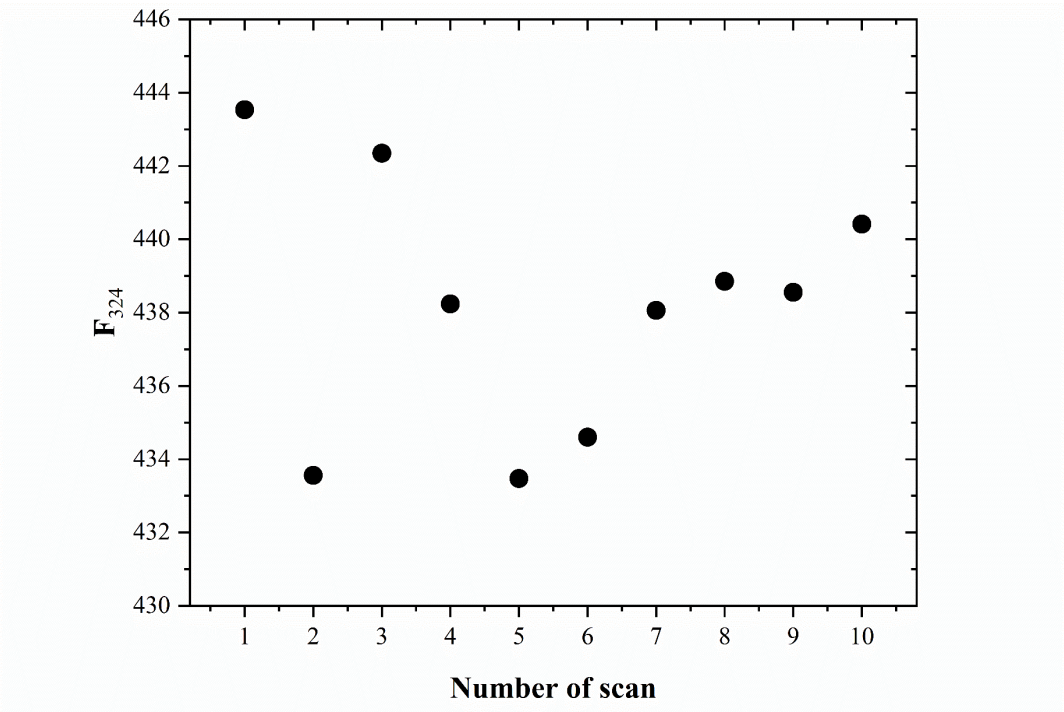

Figure S22. Fluorescence intensities at 324 nm of ten identical scans at 298 K on 15 μM [3H-***L***][OMs]$_3$ in PBS (10×, H_2O) at pH 7.0. The standard deviation (σ) of these ten measurements was 3.6.

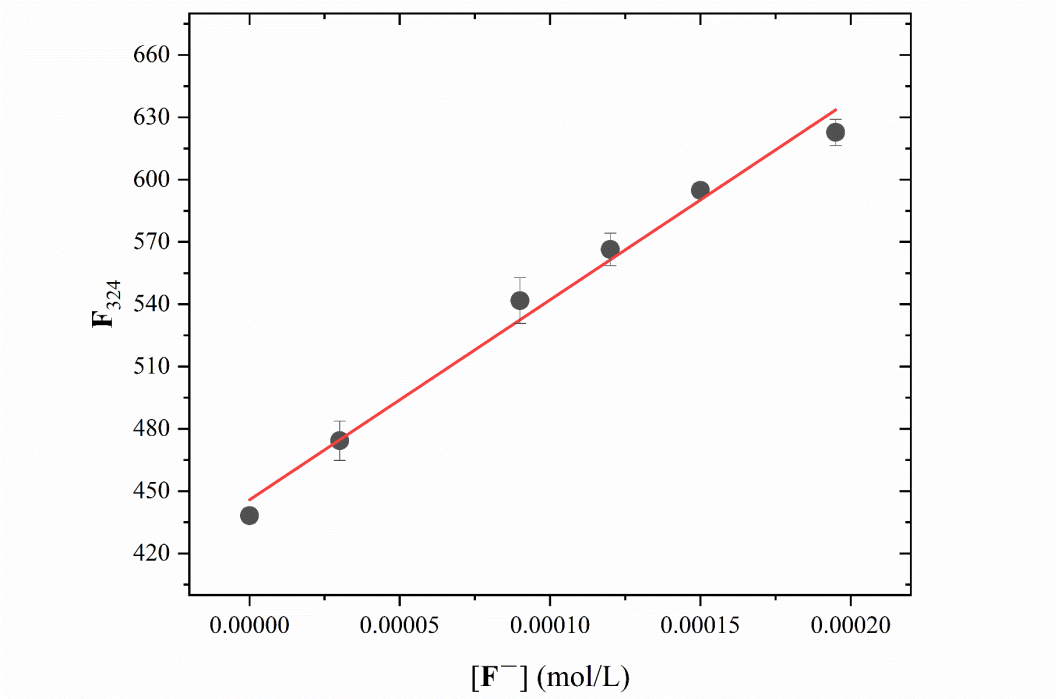

Figure S23. Fluorescence changes at 324 nm of 15 μM [3H-***L***][OMs]$_3$ versus F^- concentration at 298 K in PBS (10×, H_2O) at pH 7.0. The black spheres and red line represent experimental data and a linear fit, respectively. The error bars represent standard deviations obtained from averaging three measurements. The slope of linear calibration plot (k) was calculated to be 9.63×10^5 M^{-1} ($R^2 = 0.988$). To calculate the detection limit, equation LOD = $3\sigma/k$ was used,[6] which gave 11.2 μM.

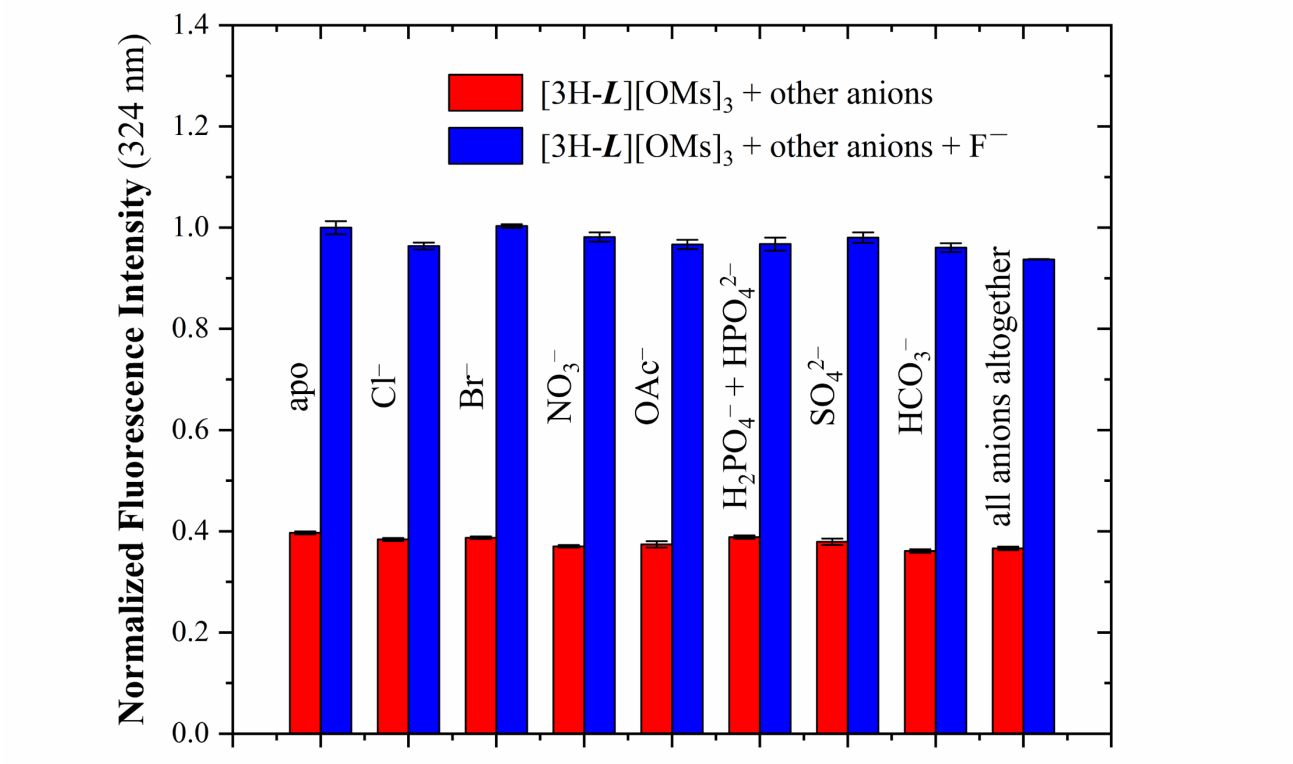

Figure S24. Fluorescence response of [3H-***L***][OMs]$_3$ to F^- in the presence of competing anions in citrate buffer (0.1 M, H_2O) at pH 7.0. The red bars show the fluorescence intensity of 15 μM [3H-***L***][OMs]$_3$ at 324 nm on the addition of respective anions (100 *eq*.). The blue bars represent the fluorescence intensity of [3H-***L***][OMs]$_3$ with 100 *eq*. F^- at 324 nm on the addition of competing anions (100 *eq*.). The error bars represent standard deviations obtained from averaging three measurements.

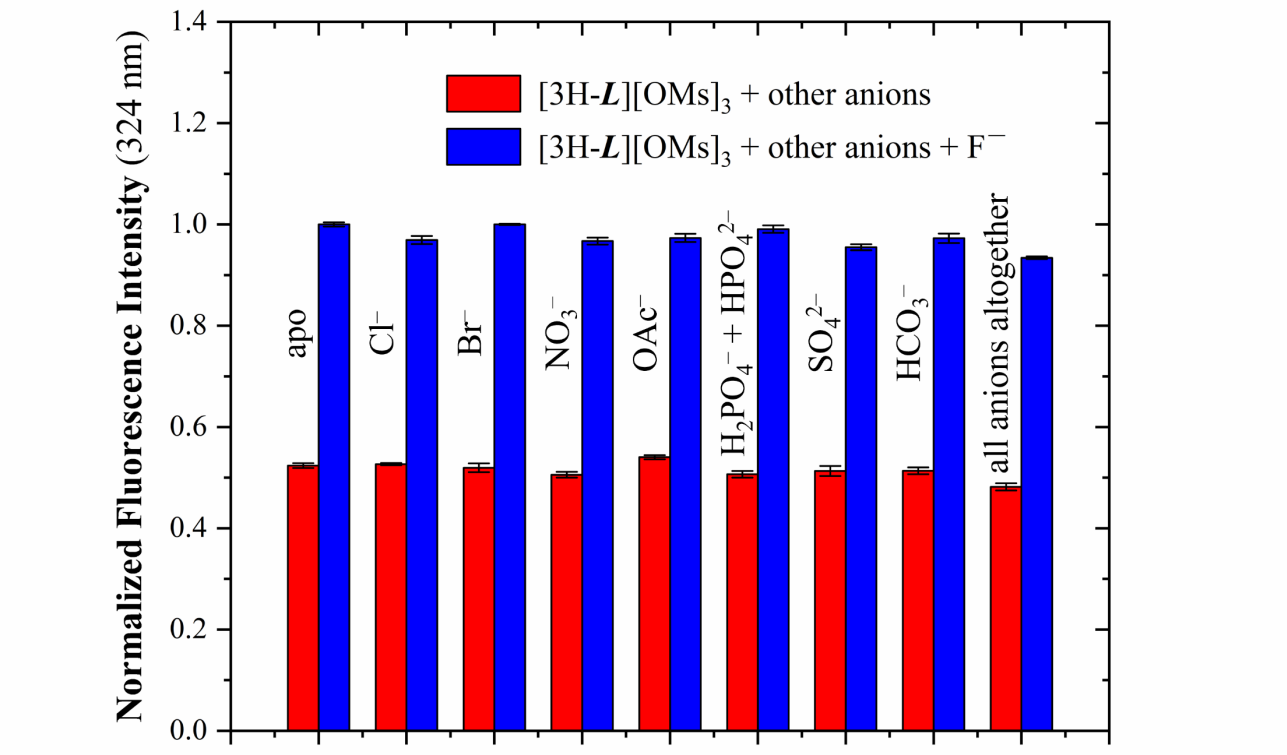

Figure S25. Fluorescence response of [3H-***L***][OMs]$_3$ to F^- in the presence of competing anions in PBS (10×, H_2O) at pH 7.0. The red bars show the fluorescence intensity of 15 μM [3H-***L***][OMs]$_3$ at 324 nm on the addition of respective anions (100 *eq*.). The blue bars represent the fluorescence intensity of [3H-***L***][OMs]$_3$ with 100 *eq*. F^- at 324 nm on the addition of respective competing anions (100 *eq*.). The error bars represent standard deviations of averaging three measurements.

UV-vis Concentration Calibration

Stock solutions of [3H-***L***][OMs]$_3$ in H_2O were sequentially diluted, adjusted to pH 5.0 ± 0.1 using a concentrated aqueous solution of methanesulfonic acid or sodium hydroxide, and their UV-vis spectra recorded at 298 K. Calibration curve intercepts were set to zero.

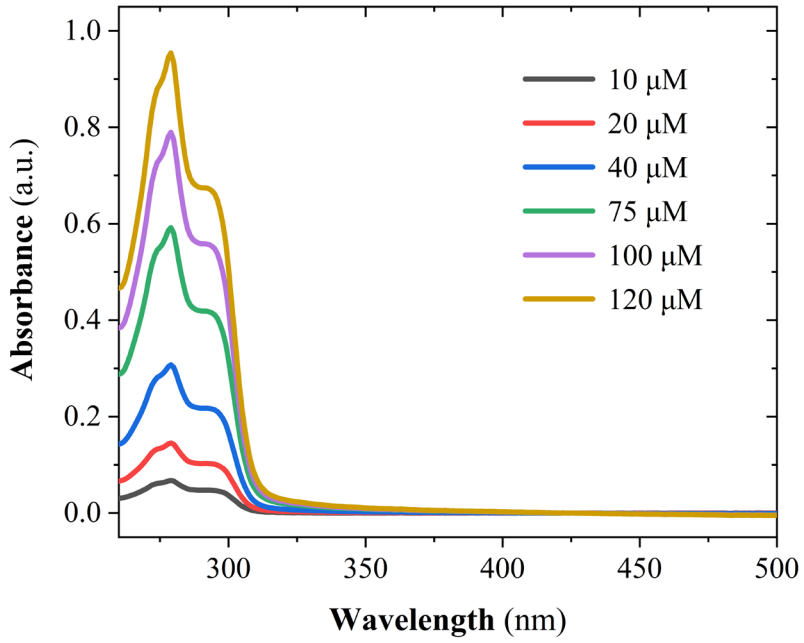

Figure S26. UV-vis spectra (pH 5.0 ± 0.1, 298 K) of [3H-***L***][OMs]$_3$ in H_2O, in the concentration range 10–120 μM.

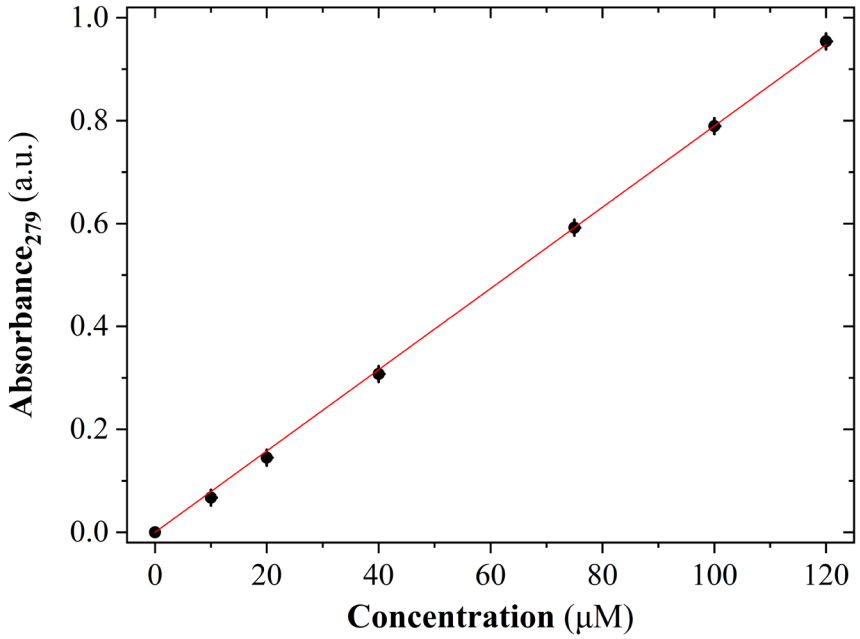

Figure S27. Concentration calibrations for [3H-***L***][OMs]$_3$ in the range 10–120 μM at pH 5.0 ± 0.1 under ambient temperature. The black spheres and red line represent experimental data and a linear fit ($y = 0.0079x$, $R^2 = 0.99979$), respectively. The error bars represent standard deviations obtained from averaging three measurements.

Immobilization of Capsules on Silica Support

The amount of material adsorbed to the silica gel (40–63 µm, 230–400 mesh, SILICYCLE) was determined by the solution depletion method. Known masses of silica were added to a series of [3H-***L***][OMs]$_3$ solutions of known concentrations and volumes. The pH of the mixture was adjusted to the desired range (± 0.1) using a concentrated aqueous solution of methanesulfonic acid or sodium hydroxide. The sample was then equilibrated *via* magnetic stirring at 250 rpm for 1 h and centrifuged at 14,000 rpm for 5 min. The concentration of the supernatant solution was determined from the UV-vis absorbance at 279 nm using the UV-vis calibration curve that was determined in the previous section. The depletion of material from solution was attributed to adsorption on the silica support.

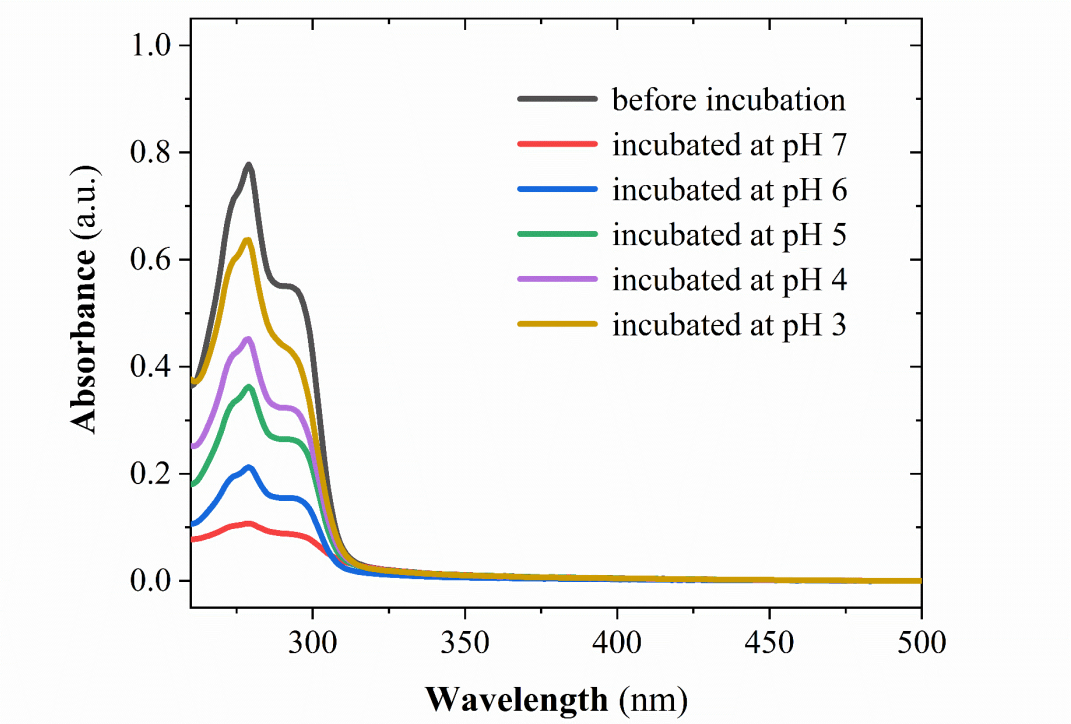

Figure S28. UV-vis spectra of the supernatant solutions before and after an aqueous solution of [3H-***L***][OMs]$_3$ was incubated with the same amount of silica gel under different pH at 298 K for 1 h.

Adsorptive Removal of Fluoride on Silica Support

To a solution of 28.5 mg/L (1.4 mmol/L) NaF in 2.5 mL D_2O was added 300 mg of silica with adsorbed capsule [3H-***L***][OMs]$_3$ (2.3 μmol). The pH of the mixture was adjusted to 5.0 ± 0.1 using a concentrated D_2O solution of methanesulfonic acid or sodium hydroxide. The sample was then equilibrated *via* magnetic stirring at 250 rpm for 1 h and centrifuged at 14,000 rpm for 5 min. The fluoride concentration of the solution was determined using ^{19}F NMR spectroscopy by adding hexafluoroacetone as the external reference. The depletion of fluoride from solution was attributed to adsorption on solid support.

Recycling the Capsules from Silica Support

To a suspension of the silica with adsorbed capsule [3H-***L***][OMs]$_3$ and fluoride in 20 mL DI water was added 20 mL $CHCl_3$. The pH of the mixture was adjusted to 12.0 ± 0.1 using a concentrated aqueous solution of methanesulfonic acid or sodium hydroxide. The sample was then equilibrated *via* magnetic stirring at 250 rpm for 1 h and centrifuged at 14,000 rpm for 5 min. The identity of the compound extracted to the organic layer was confirmed by ^1H NMR spectroscopy as the neutral form of the capsule ***L***.

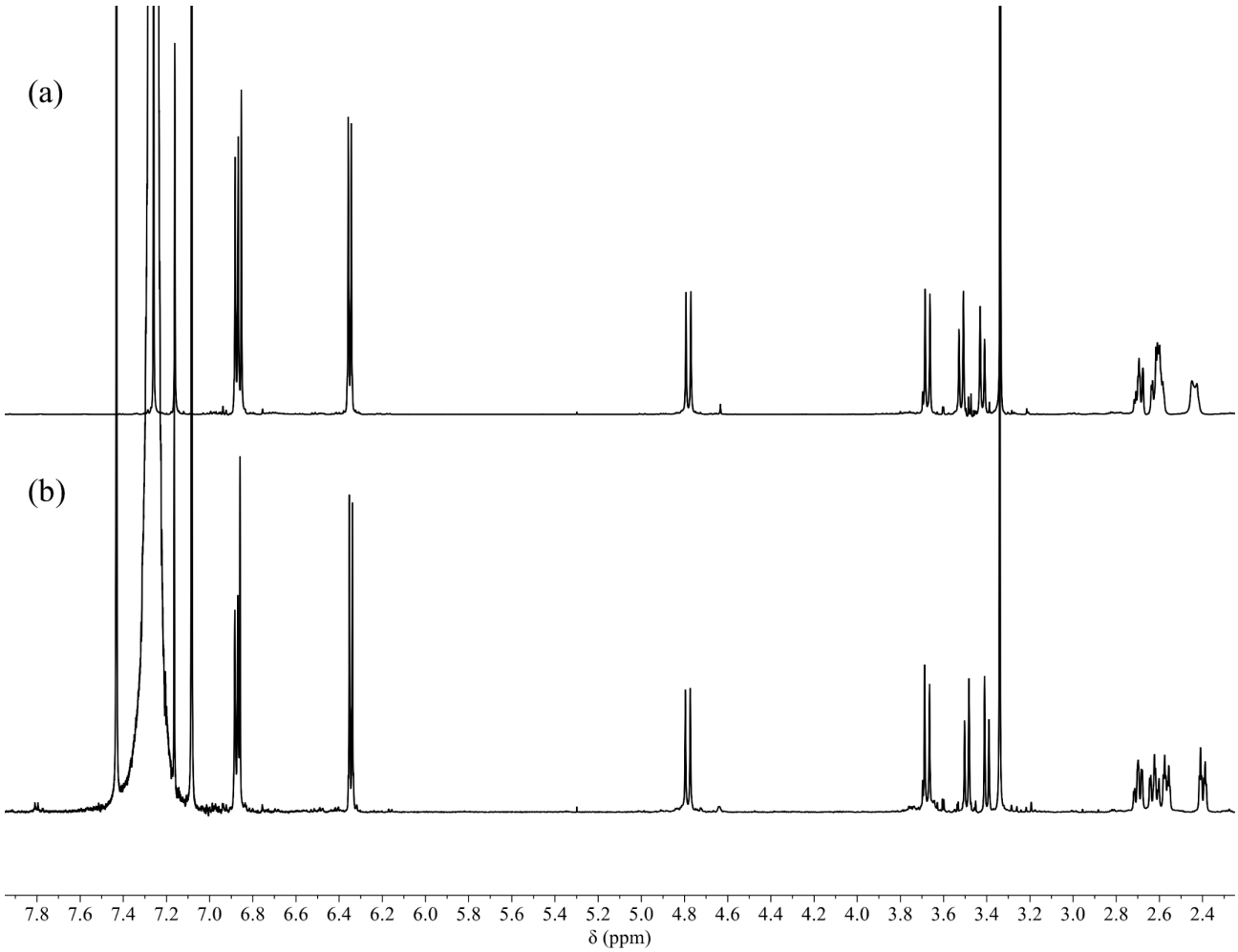

Figure S29. ^1H NMR spectra (600 MHz, 298 K, $CDCl_3$) of (a) pure ***L***; (b) the compound in the organic layer.

References

1 Y. Lin, M. R. Gau, P. J. Carroll and I. J. Dmochowski, *J. Org. Chem.*, 2022, **87**, 5158–5165.

2 P. Aru Hill, Q. Wei, T. Troxler and I. J. Dmochowski, *J. Am. Chem. Soc.*, 2009, **131**, 3069–3077.

3 G. M. Sheldrick, *Acta Crystallogr. Sect. A Found. Crystallogr.*, 2015, **71**, 3–8.

4 A. L. Spek, *Acta Crystallogr. Sect. D Biol. Crystallogr.*, 2009, **65**, 148–155.

5 G. M. Sheldrick, *Acta Crystallogr. Sect. C Struct. Chem.*, 2015, **71**, 3–8.

6 S. Amharar and A. Aydogan, *Dye. Pigment.*, 2022, **197**, 109918.